



# Application of cooling curve analysis in solidification pattern and structure control of grey cast irons

Iulian Riposan<sup>1</sup> · Mihai Chisamera<sup>1</sup> · Stelian Stan<sup>1</sup>

Received: 27 July 2017 / Accepted: 17 January 2018 / Published online: 25 January 2018  
© Akadémiai Kiadó, Budapest, Hungary 2018

## Abstract

Commercial cast iron is a typical multi-phase, natural metal matrix composite, including a ferrous matrix at different alloying grade and several phases, each having varying levels of carbon and other elements present, such as carbide, graphite and nitride. It was found that some active elements, such as S, O, Al, Ca, Ba and RE (rare earth), are important to control carbide/graphite phase formation. A major purpose of the present paper was to investigate the solidification pattern and structure of un-inoculated and inoculated cast irons, with intentionally critical conditions for graphite nucleation, typical for electric melted iron, by thermal (cooling curve) analysis technique; this is especially pertinent to the production of thin section iron castings. Increased chill (carbides formation), undercooled graphite amount, eutectic cells count and relative density correlate well with the degree of eutectic undercooling, at the beginning of eutectic reaction and at the end of solidification. Inoculation application led to decrease of  $\Delta T_m$  and increase of  $\Delta T_1$  (it became positive) and  $\Delta T_3$  (less negative) parameters, at higher influencing power on  $\Delta T_1$  parameter (narrow variation range). Higher inoculant addition rate gives better cooling curve analysis parameters.  $\Delta T_1$  appears to be the recommended cooling curve analysis parameter to characterize the specifics of solidification pattern and structure formation on the entire solidification range.

**Keywords** Grey cast iron · Solidification · Eutectic undercooling · Inoculation · Thermal analysis · Cooling curves · Structure · Carbides · Graphite · Eutectic cells

## Introduction

Cast iron is more than 70% of the total world metal casting production [more than 70 million tons of castings each year], with a great development potential. This material is especially attractive to the automotive industry, because of its excellent properties such as castability, machinability, heat conductivity and vibration damping capacity, at low production cost. Thin-wall iron castings [less than 5 mm wall thickness] are more and more attractive in this field. Industrial cast iron is a multi-element [more than 30 elements usually present] eutectic alloy. The crystallization conditions are significantly different from that of equilibrium phase diagram measured at a very slow cooling rate, using very pure materials, under vacuum melting, etc. Non-

equilibrium solidification conditions, typically for iron castings in foundry industry, favour stable to metastable system crystallization transition, austenitic dendrites formation also in eutectic-hypereutectic chemical composition ranges (Fig. 1) [1] elements segregation, different eutectic solidification undercooling [up to 50 °C or more], etc.

Commercial cast iron is a typical multi-phase, natural metal matrix composite, including a ferrous matrix at different alloying grade and several phases, each having varying levels of carbon and other elements present, such as carbide, graphite and nitride (Figs. 2 and 3). Cementite has the highest hardness ( $\sim 660$  HB), while graphite is a relatively soft, low-density material, which can act as a lubricant. Hardness, machinability, strength, ductility, toughness, thermal properties of the as-cast structure all are therefore influenced by the relative amounts of cementite and graphite. So, high-efficiency metallurgical methods need to be investigated, to control solidification pattern of iron castings, especially in critical solidification conditions.

✉ Stelian Stan  
constantin.stan@upb.ro

<sup>1</sup> Politehnica University of Bucharest, 313 Spl. Independentei, RO-060042 Bucharest, Romania

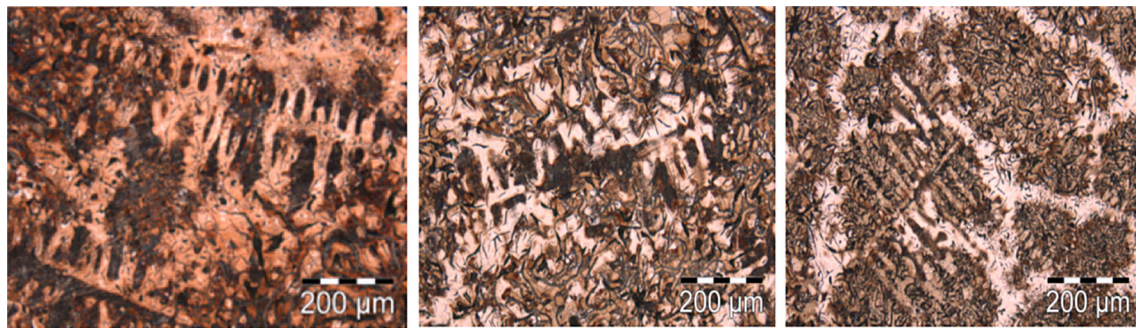


**Fig. 1** Dendritic structure in 4.4-4.5 mass% CE grey cast irons ( $\text{CuCl}_2$ -base solution etchant)

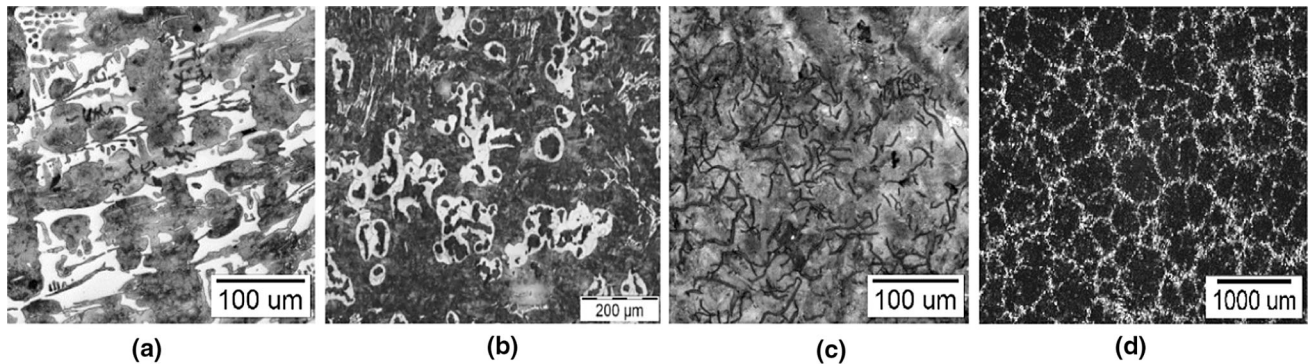


**Fig. 2** Cast iron—natural metal matrix composite [a pearlite + graphite + carbides; b pearlite + ferrite + graphite + carbides; c pearlite + graphite + phosphide; d eutectic cells]

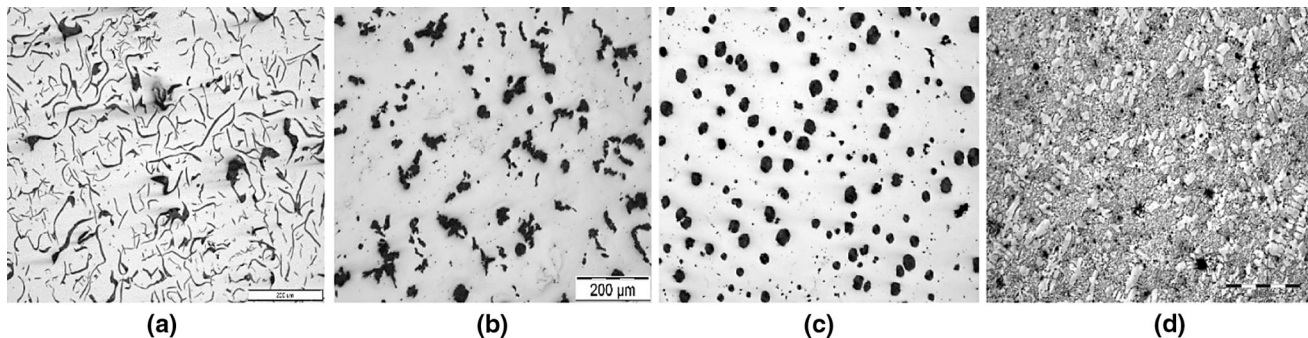


**Fig. 3** Typical graphite morphologies in cast irons [a lamellar; b vermicular/compacted; c nodular/spheroidal; d coral]

Graphite nucleation sites formation as size, distribution and morphology and their growth pattern to obtain different final graphite morphologies (lamellar/flake, vermicular/compacted or nodular/spheroidal) could be influenced by modification and/or inoculation treatments. Higher graphite particles compactness degree [from lamellar through compacted up to spheroidal form] lowers their capacity for stress concentration and as result, improves all of the mechanical properties level, especially ductility.

Inoculation is a graphitizing treatment of the molten iron, applied to all of cast irons, in order to obtain an as-cast structure without carbides and with high-quality graphite shape (the best-expected graphite morphology

specifically for each cast iron type). It consists in addition of 0.05...1.0 mass% inoculant in the final molten iron as it is transferred [1300...1500 °C]. Inoculants are  $\text{FeSiAlX}$  alloys, where  $X = \text{Ca, Ba, Sr, Zr, RE}$ , as well-known inoculating elements that promote and participate in the creation of micron-sized active compounds in the iron melt, to act as effective graphite nucleation sites [2].

The routine measurements of metallurgical treatments effects in a foundry are in many ways empirical and have to be calibrated as well as interpreted to have any value in managing the process. It is well known that chemical analysis results from a spectrometer sometimes do not reflect the truth or match other benchmark test values. With

**Table 1** Dimensions of standard test wedges (ASTM A367)

Wedge no.	Wedge dimensions/mm			Angle/deg/A	Calculated parameters	
	Width/B	Height/H	Length/L		Wedge section area/mm <sup>-2</sup>	Cooling modulus/cm
W <sub>1</sub>	5.1	25.4	101.6	11.5	67.3	0.11
W <sub>2</sub>	10.2	31.8	101.6	18.0	162.2	0.21
W <sub>3</sub>	19.1	38.1	101.6	28.0	354.3	0.35
W <sub>3½</sub>	25.4	44.4	127.0	32.0	563.9	0.45
W <sub>4</sub>	31.8	50.8	152.4	34.5	807.7	0.54

the more widespread adoption of thermal analysis testing, thermal analysis data have become an indicator of iron quality [3–19].

As it was found that some active elements, such as sulphur, oxygen, aluminium, calcium, barium and rare earth (RE), are important to control in situ carbide/graphite phase formation in cast iron matrix composite material [20–33], a major purpose of the present paper was to investigate the solidification pattern and structure of uninoculated and inoculated cast irons, with intentionally critical conditions for graphite nucleation, typical for electric melted iron, by thermal (cooling curve) analysis technique; this is especially pertinent to the production of thin-section iron castings.

## Experimental

Base cast iron with controlled and low level of sulphur (< 0.03 mass% S) and aluminium (< 0.002 mass% Al) in hypoeutectic range (3.6–3.8% carbon equivalent–CE, 0.6–0.7 mass% Mn) was prepared in coreless induction furnace (acid lining, 1500 kg capacity, 250 Hz) from selected steel scrap, graphitic recarburiser, low aluminium ferrosilicon and FeMn. Lower level of sulphur and aluminium should provide a cast iron more prone to type-D graphite and carbides formation [20, 24, 30, 32].

Two systems of representative commercial FeSi-based inoculants were used, employing Ca and Ba (1.0–2.5 mass% Ca and 1.0–2.5 mass% Ba) or rare earth (RE) and Ca (1.5–2.0 mass% RE and 1.0–1.5 mass% Ca) as the inoculating elements. The alloy had a 0.2–0.7 mm particle size range. Inoculant was added at two levels of 0.15 and 0.25 mass% into the pouring ladle during tapping. Each un-inoculated and inoculated iron batch was held for 2.0–2.5 min before pouring in furan resin moulds. Standard 30 mm bars, usually used for structure characterization of grey iron castings, were considered.

The present experiments focused on the high cooling/solidification rate W<sub>1</sub>, W<sub>2</sub> and W<sub>3</sub> samples—ASTM A

367 (furan resin mould), characterized by Table 1 data. [10, 34] A large range of castings are represented by considering these wedge-shaped samples. Thin-wall castings are represented by the highest cooling rate W<sub>1</sub> wedge, while the W<sub>2</sub> and W<sub>3</sub> samples reflect medium cooling rate solidification.

The solidification process was investigated by Quick-cup<sup>TM</sup> cooling curve analysis having a modulus of approximately 0.75 cm (equivalent to 30-mm diameter bar). The cooling curve [ $T = f(\tau)$ ] and its first derivative [ $dT/d\tau = f'(\tau)$ ] were recorded (Fig. 4) [9].

## Results and discussion

The cooling curve, and its derivatives, displays patterns that can be used to predict the characteristics of a cast iron, according to Fig. 4. The significance of the most important events and parameters on these curves refers to the equilibrium temperatures in the stable (T<sub>st</sub>) and metastable (T<sub>mst</sub>) systems. The thermal analysis evaluation mainly considered some important temperatures on the cooling curves of hypoeutectic grey cast irons, such as TAL—temperature of the austenite liquidus (zero point on the first derivative), TSEF—temperature of the start of eutectic freezing (minimum negative on the first derivative at the beginning of solidification), TEU—the lowest eutectic temperature (zero point on the first derivative) and TES—temperature of the end of solidification (minimum on the first derivative at the end of solidification).

Melting procedure [superheating and holding, temperature and time], inoculation procedure [inoculating elements, inoculant type and amount, inoculation technique] and solidification procedure [casting thickness and cooling modulus, mould media and their thermo-physical properties] usually affect the solidification cooling curve and its first derivative parameters.

The present work focuses on the influence of the inoculating elements [inoculant system] and inoculant addition amount, for controlled pouring parameters and constant solidification conditions [standard ceramic mould, 0.73 cm

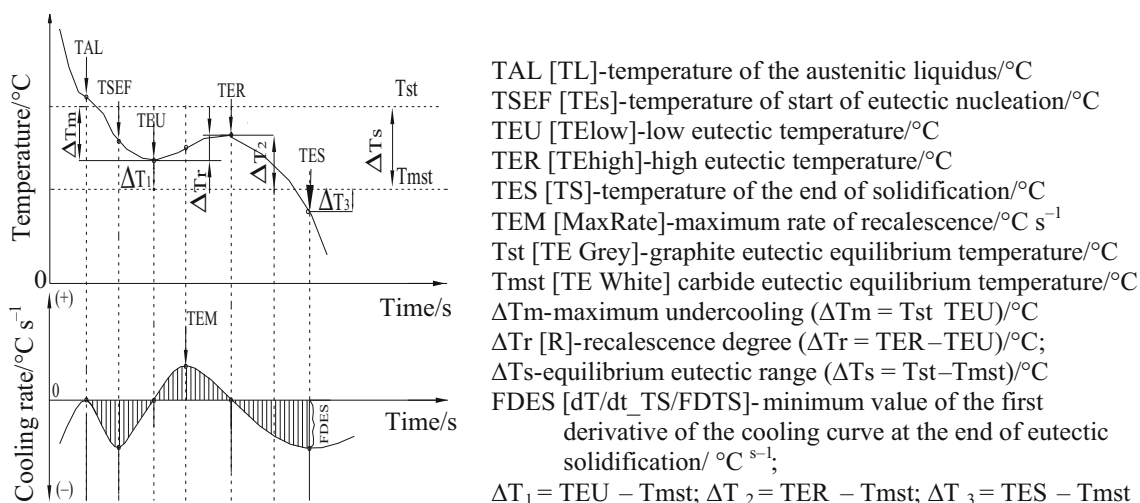


Fig. 4 Thermal analysis—nomenclature and units for a hypoeutectic cast iron

cooling modulus]. Figure 5 illustrates the effects of the selected influencing factors [inoculant system and addition amount] on the selected thermal analysis parameters [ $\Delta T_m$ ,  $\Delta T_1$ ,  $\Delta T_3$ ] (see Fig. 4) and their relationships, respectively.

When TEU (temperature of maximum eutectic undercooling) is reached, the combined heat generated from the release of specific heat and latent heat (from the first austenite dendrite solidification and latent heat from the start of eutectic freezing) just balances the heat losses. The eutectic reaction then occurs, and the released energy causes the temperature to rise until TER (temperature of eutectic recalescence) is reached. The lowest eutectic temperature (TEU) is strongly influenced by inoculation, as a graphitizing treatment, and, consequently, the eutectic undercooling degrees at this beginning of eutectic reaction, too, refer to the stable (graphitic) eutectic temperature ( $\Delta T_m = T_{st} - TEU$ ) or metastable (carbide) eutectic temperature ( $\Delta T_1 = TEU - T_{mst}$ ). These temperatures were calculated using the chemical composition, mainly silicon [ $T_{st} = 1153 + 6.7\% \text{ Si}$ ;  $T_{mst} = 1147 - 12\% \text{ Si}$ ] [8].

The present study describes the effect of Ca, Ba-FeSi and RE, Ca-FeSi alloys at an addition rate of 0...0.25 mass% on thermal analysis parameters and cast iron characteristics (structure and contraction defects sensitivity). According to low level of carbon equivalent (CE = 3.6–3.8%), combined with low content of sulphur (< 0.03%) and residual aluminium (< 0.002%), and high superheating procedure, typically for electric melting, the tested irons are characterized by high eutectic undercooling in un-inoculated condition ( $\Delta T_m > 38$  °C,  $\Delta T_1 < 0$ ). As a result, these irons are sensitive for free carbides formation and uncalled for undercooled graphite morphology, generating a need for inoculation.

Inoculation application led to decrease of  $\Delta T_m$  (more than 30%) and increase of  $\Delta T_1$  (it became positive)

parameters, favourable for better properties of cast irons, despite low inoculant amounts addition. The difference between un-inoculated and inoculated irons is strongly affected by the alloy addition rate. It means a higher inoculant amount, a higher graphitizing power, so a lower  $\Delta T_m$  (Fig. 5a) and a higher  $\Delta T_1$  (Fig. 5b), respectively, but at a higher influencing power on  $\Delta T_1$  parameter (narrow variation range). These positive effects characterize each inoculation alloy (inoculant). Rare earth bearing inoculant appears to be more active than calcium and barium bearing alloys at the lowest addition amount.

The two eutectic undercooling  $\Delta T_m$  and  $\Delta T_1$  are in good relationship (Fig. 5d), so the second one is recommended, as it illustrates clearer the solidification specific of cast irons: carbides occurrence for  $\Delta T_1 < 0$ , and undercooled graphite formation for positive, but limited level of this parameter (usually less than 15 °C). Therefore, the efficiency of inoculation is measured by its ability to decrease the  $\Delta T_m$  level and to increase the  $\Delta T_1$  levels, respectively.

The end of the eutectic solidification is also very important, especially because the micro-shrinkage occurs at the latter part of solidification, usually at hot spots or parts with a large cooling modulus. White iron solidification as intercellular carbides and/or inverse chill formation is also dependent on the position of the temperature at the end of solidification (TES), compared to the metastable (white) eutectic temperature ( $T_{mst}$ ), expressed by  $\Delta T_3$  undercooling parameter (Fig. 4). TES solidus temperature is an important parameter that is sensitive to certain elements. This point can be found at the latest part of the first derivative, as the lowest of the negative peak. Higher TES (less negative) leads to a lower tendency for intercellular carbides (inverse chill), and micro-shrinkage defects at the end of solidification.

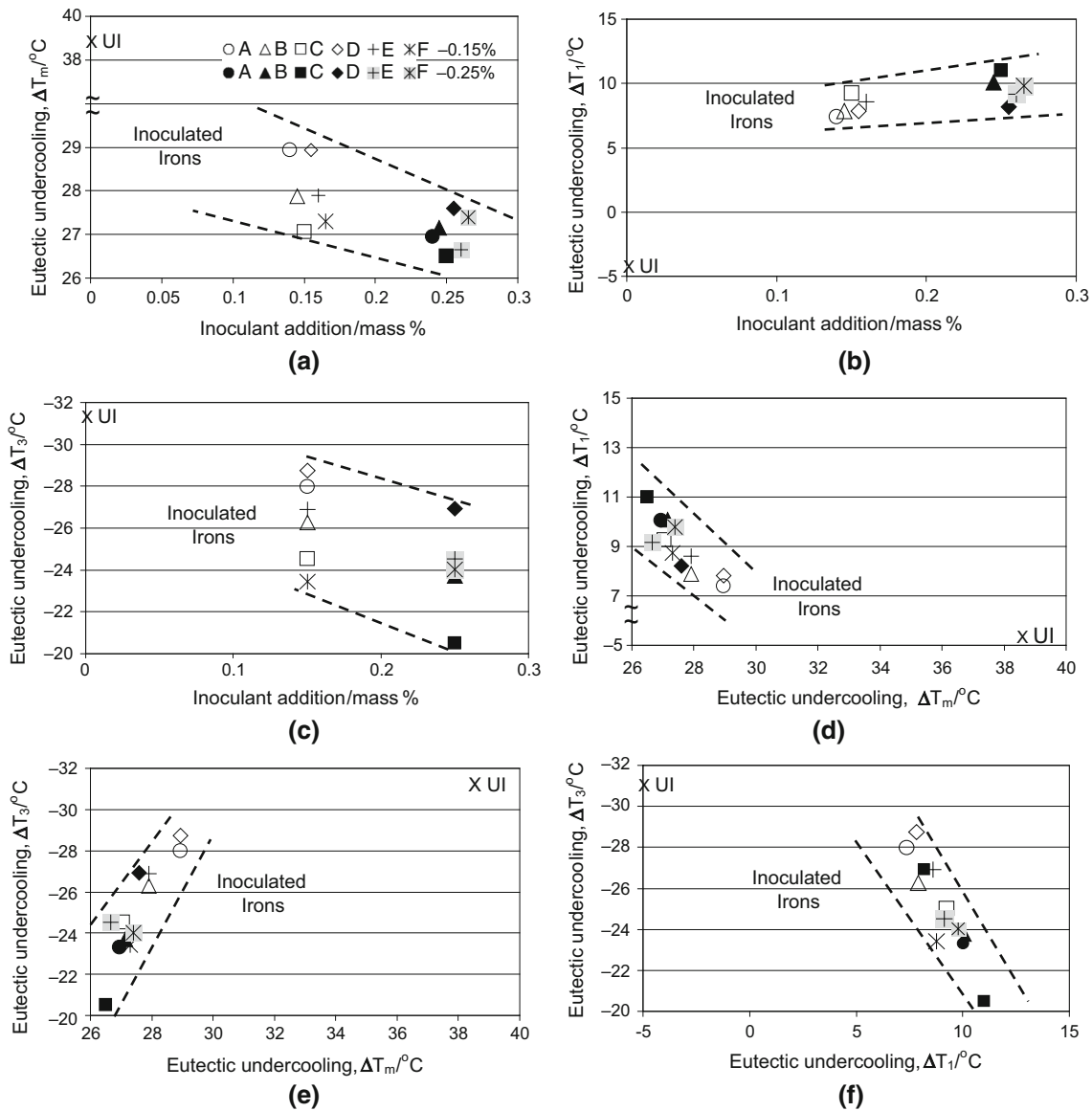


**Fig. 5** Influence of inoculant addition amount on the eutectic undercooling  $\Delta T_m$  **a**,  $\Delta T_1$  **b**,  $\Delta T_3$  **c** and their relationships **d**, **e**, **f**. [A...E-Ca, Ba-FeSi alloys; F-RE, Ca-FeSi alloy; UI un-inoculated irons]

Because this difference ( $\Delta T_3$  parameter) is more than  $30^\circ\text{C}$  (Fig. 5c), un-inoculated iron will be sensitive to chill tendency and micro-shrinkage formation. A preferred end of solidification means high solidus temperature and low level (less negative) of the  $\Delta T_3$  parameter (usually as low negative value, as  $\text{TES} < \text{Tmst}$  in most cases). Figure 5c shows that the solidification pattern of inoculated irons is more favourable compared to that of un-inoculated irons. Increasing the alloy addition improves the behaviour of irons at the end of solidification ( $\Delta T_3$  became less negative), with a relative large dependence on the inoculant type. It is expected that each commercial inoculant could have different behaviour, depending on inoculating elements presence, their ratio into alloy

chemistry and inoculant amount addition. It appears that for the present critical production conditions (low carbon equivalent and very low sulphur and aluminium content, and high superheating in melting furnace), rare earth bearing inoculants could be a solution at low addition rate.

Undercooling degree at the end of solidification ( $\Delta T_3$ ) is in good relationship with the maximum eutectic undercooling at the beginning of eutectic reaction, expressed by its reference to stable eutectic temperature ( $\Delta T_m$ , Fig. 5e) and metastable eutectic temperature ( $\Delta T_1$ , Fig. 5f), respectively. It is important for practical application, and  $\Delta T_1$  measured by controlled metastable (carbide) solidification (Te addition ceramic cup). It was found that  $\text{Tmst}$

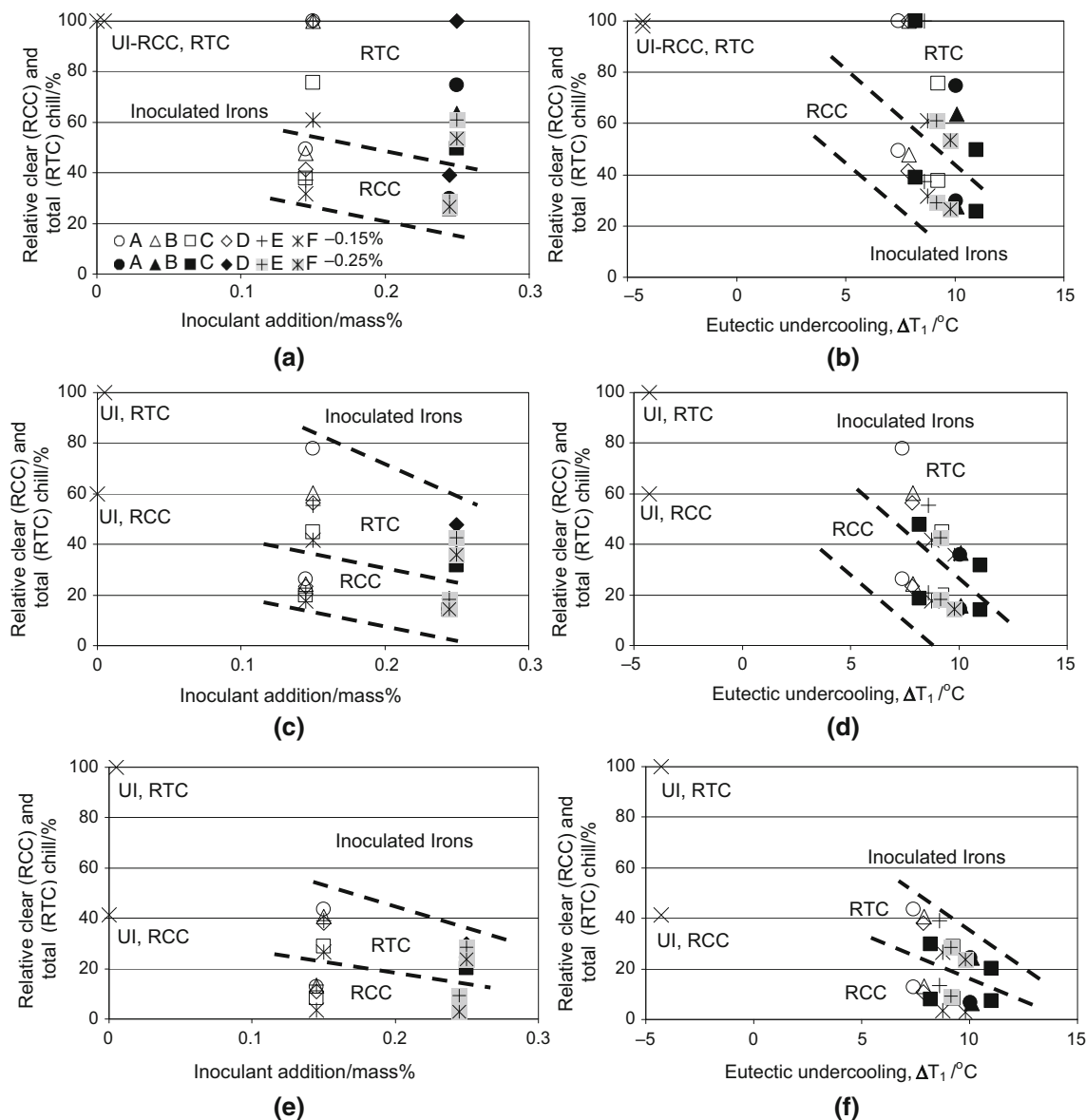


**Fig. 6** Influence of inoculant addition amount (a, c, e) and eutectic undercooling  $\Delta T_1$  (b, d, f) on the relative clear (RCC) and total (RTC) chill of  $W_1$  (a, b),  $W_2$  (c, d) and  $W_3$  (e, f) ASTM A 367 wedge samples [A...E-Ca, Ba-FeSi alloys; F-RE, Ca-FeSi alloy; UI un-inoculated irons]

evaluation by this way is more exact compared to calculus on the base of chemical composition of cast iron. [16]

Wedges of the type  $W_1$ ,  $W_2$  and  $W_3$  specified in the ASTM A367 wedge test were used to evaluate the cast irons sensitiveness for chill [carbides] formation, with detrimental effects on mechanical, thermal and machining properties. Table 1 shows the size and calculated cooling modulus of tested wedges. The average cooling rates in the solidification range in the wedge thermal centre also differentiate the solidification pattern of these castings:  $3.0\text{ }^\circ\text{C}$  for  $W_1$ ,  $1.75\text{ }^\circ\text{C s}^{-1}$  for  $W_2$  and  $0.75\text{ }^\circ\text{C s}^{-1}$  for  $W_3$  wedge, respectively. [10]

The chilled iron at the apex of the wedge consists of different zones. The portion nearest the apex, entirely free

of grey areas, is designated as the clear chill zone (CC). The portion from the end of the clear chill zone to the location where the last presence of cementite, or white iron is visible, is designated the mottled zone (MC). The region from the junction of grey fracture to the first appearance of chilled iron (apex) is designated the total chill (TC). The parameters relative clear chill (RCC) and relative total chill (RTC) were considered [35]:

$$\text{RCC} = 100 [\text{CC}/\text{B}] (\%) \quad (1)$$

$$\text{RTC} = 100 [\text{TC}/\text{B}] (\%) \quad (2)$$

where B is the maximum width of the test wedge (Table 1).

Macro-structures of the fractured wedge samples, representing un-inoculated iron and irons inoculated at two

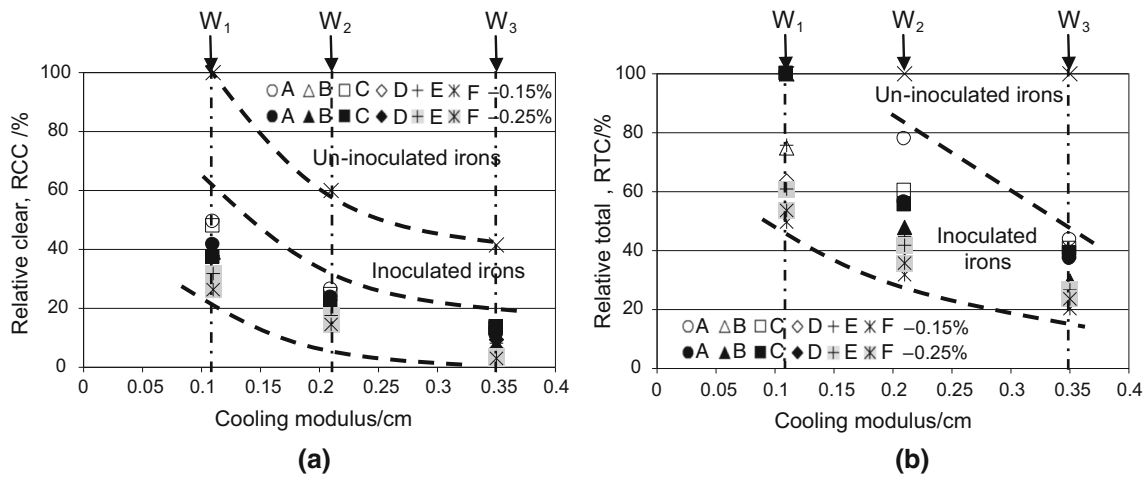
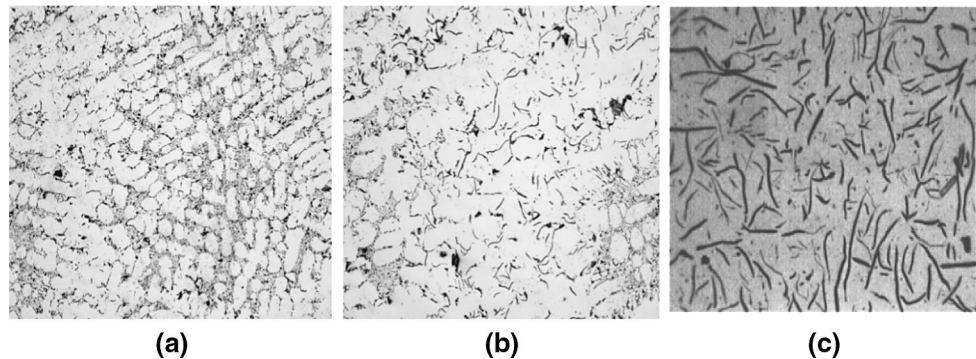


**Fig. 7** Influence of solidification cooling modulus of wedge castings [ASTM A 367] on the relative clear chill (RCC, a) and relative total chill (RTC, b), of un-inoculated (UI) and inoculated irons (A...E-Ca, Ba-FeSi alloys; F-RE, Ca-FeSi alloy)

**Fig. 8** Lamellar graphite morphology in grey cast irons [a undercooled graphite, type D; b type D + type A graphite; c type A graphite] [un-etched samples]



addition levels, 0.15 and 0.25 mass% alloy, were analysed, and the characteristic zones (white, mottled and grey areas) were measured. Relative clear chill (RCC, Eq. 1) and relative total chill (RTC, Eq. 2) were calculated. Figures 6 and 7 graphs illustrate the effect of treatment (un-inoculated and inoculated irons), inoculant amount addition (0.15 and 0.25 mass%) and inoculant system (Ca, Ba-FeSi and RE, Ca-FeSi alloys), wedge test type (cooling modulus and cooling rate) and chill sensitiveness evaluation criteria (RCC and RTC). Correlation between chill (carbides) tendency and representative thermal analysis parameters was also considered. Figure 6b, d, f illustrates the relationship of chill and eutectic undercooling at the beginning of eutectic reaction ( $\Delta T_1$ ). Both cooling rate and inoculation are important influencing factors.

Un-inoculated irons are characterized by having high chilling tendency, for all of tested solidification conditions. Inoculation gave, as expected, overall lower iron chill than with no inoculation, even at lower inoculant (0.15 mass%) in-ladle additions. A 0.15 mass% inoculant addition had a very big influence on chill tendency compared to un-inoculated irons, especially at the higher cooling rate (or lower cooling modulus of wedge samples).

According to generally accepted understanding of the effects of inoculants, despite the limited action to change to the base iron carbon equivalent, inoculation resulted in a strong decrease in chill tendency. This shift was more pronounced for 0.15 mass% inoculation relative to the base iron, than with an increased alloy addition rate from 0.15 to 0.25 mass%.

A number of trends in chill sensitivity could be identified. At low cooling modulus, or thin-wall solidification, respectively, the inoculation efficiency is higher, referring to un-inoculated irons, compared to lower cooling rate solidification. In general, as can be seen in Figs. 6a,c,e and 7, chill tendency decreased with increasing cooling modulus (CM)/decreasing of cooling rate, but with some differences, depending on whether the iron was un-inoculated or inoculated and also depending on the chill criteria (clear chill and total chill). The difference between un-inoculated and inoculated irons increases, from clear chill up to total chill, especially for higher solidification rates. The difference in total chill is larger than with clear chill. Iron melt inoculation, especially at a higher addition rate, had an important homogenizing effect on the solidification behaviour of castings in the chill evaluation.

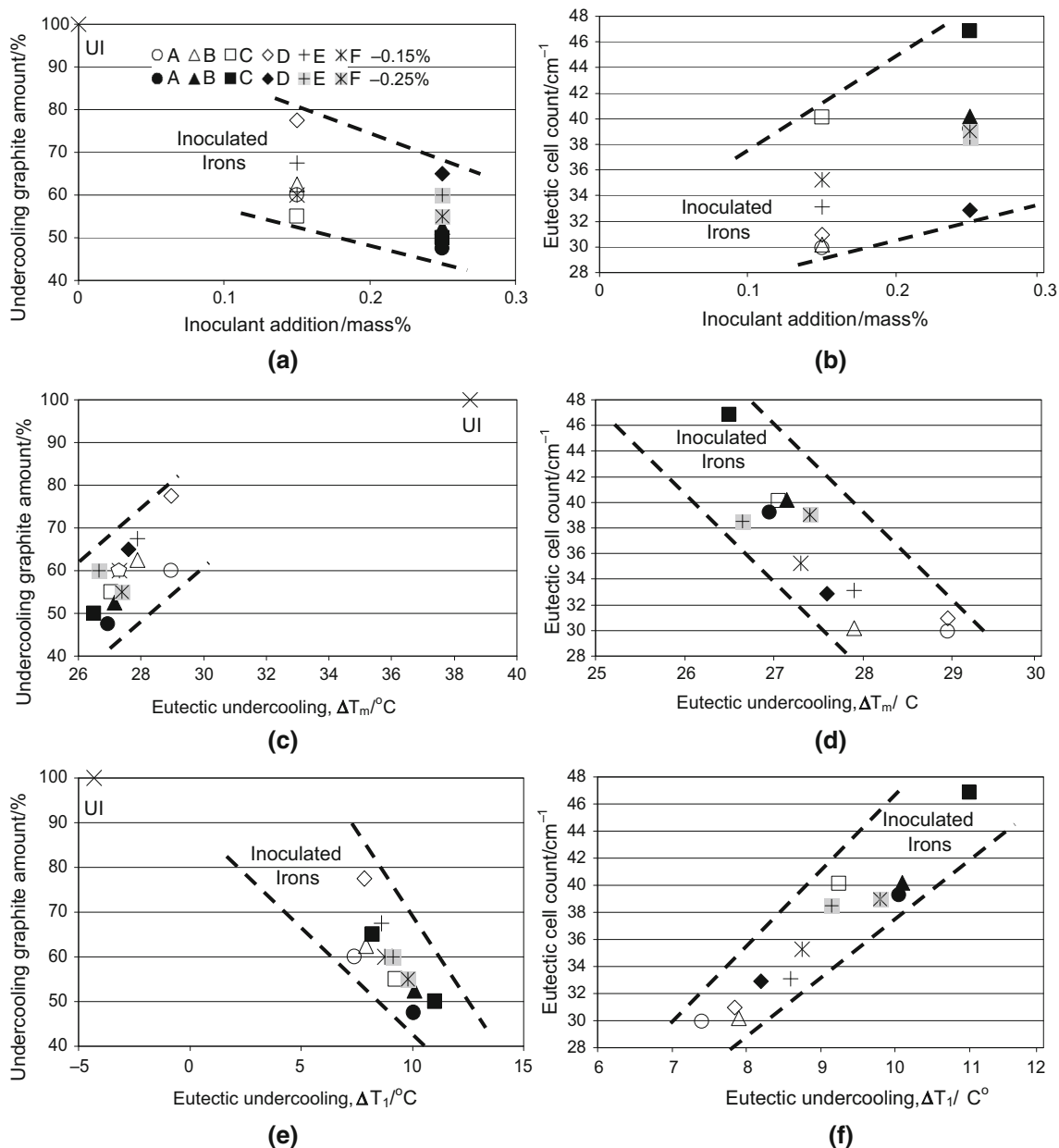


**Fig. 9** Influence of inoculant addition amount (a, b) and eutectic undercooling (c, d, e, f) on the undercooled graphite amount (a, c, e) and eutectic cell count (b, d, f) [A...E-Ca, Ba-FeSi alloys; F-RE, Ca-FeSi alloy; UI un-inoculated irons]

The efficiency of the inoculation treatment is seen to depend on the cooling rate of the castings (CM) and evaluation criteria, respectively. Total chill reached 100% in un-inoculated irons for all of cooling modulus solidification conditions. A 0.15 mass% inoculant addition led to a relative clear chill value, at the highest cooling rate ( $W_1$  wedge), comparable to un-inoculated iron solidified at medium cooling rate ( $W_2$  wedge). Inoculant system appears to be important, as chill tendency of rare earth bearing FeSi alloy-treated irons is systematically at a lower level of all of treatment and solidification conditions.

For each cooling modulus/solidification cooling rate,  $W_1$ ,  $W_2$  and  $W_3$  castings, respectively, the relationship between chill sensitiveness and eutectic undercooling  $\Delta T_1$  parameter evaluated by thermal analysis (Fig. 6b, d, f) is stronger than the dependence between chill and inoculant amount addition (Fig. 6a, c, e). Higher  $\Delta T_1$  parameter obtained by inoculation gives low chill tendency, independently of inoculant consumption, inoculant type, solidification cooling rate and chill evaluation criteria. Generally, rare earth bearing ferrosilicon alloy led to the best results as the decreasing of carbides formation



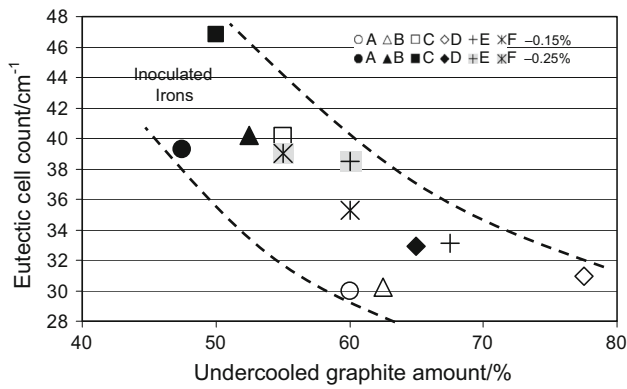


**Fig. 10** Eutectic cell count and undercooled graphite amount relationship in inoculated irons [A...E-Ca, Ba-FeSi alloys; F-RE, Ca-FeSi alloy]

sensitiveness. These results sustain the possibility to evaluate the chill (carbides formation) tendency of a specific solidified casting by thermal analysis in standard Quick-cup™ conditions.

The effects of inoculation were also analysed by comparing the microstructures of irons treated with different amounts of inoculating alloys, utilizing the 30-mm diameter bars, in visible connection with thermal analysis parameters. The influence of inoculant addition rate on the

undercooled graphite (type-D graphite, ASTM, ISO, Fig. 8a) amount and eutectic cell (see Fig. 2d) count is shown in Fig. 9.

Un-inoculated iron is extremely sensitive to undercooled graphite formation (100%), while inoculation led to lower amount of this un-wanted graphite morphology, depending on inoculant amount and type: 20–45% decreasing for 0.15 mass% inoculant and 35–55% decreasing for 0.25 mass% inoculant, respectively. Despite its better capacity to decrease carbides formation sensitiveness, rare earth bearing ferrosilicon alloy appears to have only a medium power compared to calcium and barium bearing commercial inoculants. Figure 9c and

9e shows a good relationship between undercooled graphite amount in 30-mm test bar and some thermal analysis parameters obtained in Quick-cup™ application, such as the eutectic undercooling at the beginning of eutectic reaction,  $\Delta T_m$  and  $\Delta T_1$ . Higher  $\Delta T_m$  or lower  $\Delta T_1$  gives higher sensitiveness to undercooled graphite formation.  $\Delta T_1 < 0$ , typically for un-inoculated iron, means 100% undercooled graphite. Increased  $\Delta T_1$ , but in limited level ( $0 < \Delta T_1 < 10$  °C), favoured the decreasing of undercooled graphite amount up to 50%. In the specific tested conditions, higher  $\Delta T_1$  level is necessary to limit more the occurrence of this graphite morphology.

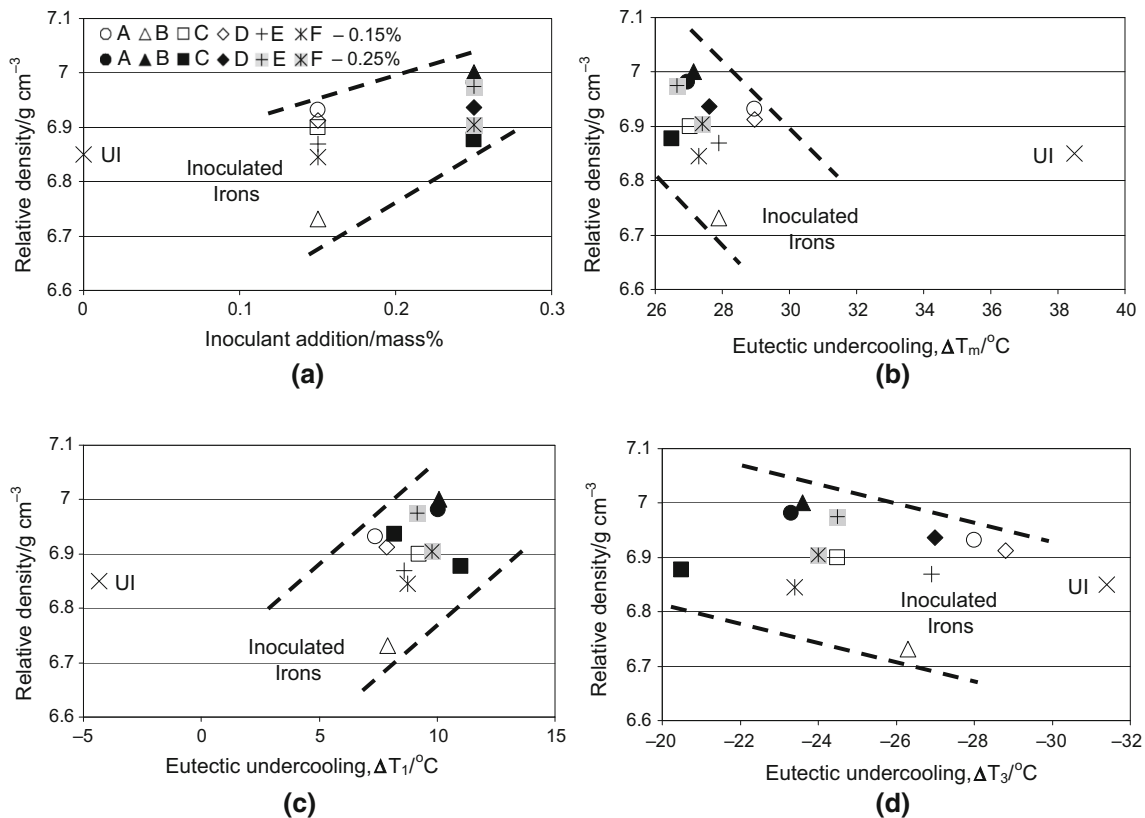


**Fig. 11** Influence of inoculant addition amount (a) and eutectic undercooling  $\Delta T_m$  (b),  $\Delta T_1$  (c) and  $\Delta T_3$  (d) on relative density [A...E-Ca, Ba-FeSi alloys; F-RE, Ca-FeSi alloy; UI un-inoculated irons]

Typically, solidification of graphitic cast iron is the eutectic cell formation. As representative member of solidification structure of cast irons, including austenite and graphite, formed during the eutectic reaction, eutectic cell will influence the properties of castings, mainly by their count and size. Higher count (lower size) gives higher the boundary area and a more favourable (less dangerous/less concentrated) distribution of the segregated phases in inter-cells regions. On the other hand, at lower size eutectic cells formation, lower graphite particles size will result. Both of these effects (lower size of eutectic cell and graphite particles) will improve the major properties of cast irons. Inoculation is usually used to activate nucleation sites of graphite and to promote graphite formation, respectively. As graphite is the leader in eutectic cells formation, higher eutectic cells count usually result. Figure 9b confirms these beneficial effects of inoculation, which is true for all of inoculants tested in this experiment. The present work illustrates the possibility to evaluate the eutectic cells count by standard thermal analysis, including the eutectic undercooling at the beginning of eutectic reaction (Figs. 9d, f). Eutectic cells count decreased by increasing of the undercooling referring to stable eutectic temperature ( $\Delta T_m$ , Fig. 9d), but increased by increasing of the undercooling referring to metastable eutectic temperature ( $\Delta T_1$ , Fig. 9f), with a good relationship rule.

The two important members of primary structure of cast irons, influenced by inoculation, undercooled graphite amount and eutectic cells count, are in inverse variation, as Fig. 10 shows: higher eutectic cells count means lower undercooled graphite amount occurrence. It is visible that the increasing of inoculant amount, which led to the decreasing of undercooled graphite amount, as result of decreasing of the eutectic undercooling referring to the stable eutectic temperature ( $\Delta T_m$ ), favours a higher eutectic cells count.

The relative density of the tested cast irons, by reporting of the samples weight to their volume was also recorded, is a simple possibility to illustrate the sensitiveness of castings to contraction defects formation (shrinkage and microshrinkage). Figure 11 shows some obtained important results in this respect. Generally, inoculation improved this parameter, as a result of improving important thermal analysis parameters, such as the undercooling at the beginning of eutectic reaction ( $\Delta T_m$ , Fig. 11b and  $\Delta T_1$ , Fig. 11c) and at the end of solidification ( $\Delta T_3$ , Fig. 11d). Higher inoculant amount addition gives higher relative density, according to lower undercooling on entire solidification range. This is generally true for all of tested commercial inoculants, with calcium and barium bearing ferrosilicon alloys, but in a relatively scattered range.

## Conclusions

Based on the results of thermal analysis of solidification process, some conclusions can be made on the effect melt inoculation has on structure at given grey iron casting parameters in critical solidification conditions, namely a relatively low carbon equivalent (CE = 3.6–3.8%), combined with low content of sulphur (< 0.03%) and residual aluminium (< 0.002%), typical for electric melting.

- (1) Increased chill (carbides formation), undercooled graphite amount and contraction defects sensitiveness correlate well with certain thermal analysis parameters, such as the degree of solidification eutectic undercooling, referring to the both stable (-graphitic) and metastable (carbide) eutectic temperature, at the beginning of eutectic reaction ( $\Delta T_m$ ,  $\Delta T_1$ ) and at the end of solidification ( $\Delta T_3$ ).
- (2) Inoculation application led to decrease of  $\Delta T_m$  (more than 30%) and increase of  $\Delta T_1$  (it became positive) and  $\Delta T_3$  (less negative) parameters, at higher influencing power on  $\Delta T_1$  parameter (narrow variation range), despite low inoculant amounts addition. Higher inoculant addition rate gives better cooling curve analysis parameters.
- (3) The two eutectic undercooling  $\Delta T_m$  and  $\Delta T_1$  are in good relationship, so the second one is recommended, as it illustrates clearly the solidification specific of cast irons: carbides occurrence for  $\Delta T_1 < 0$ , and undercooled graphite formation for positive, but limited level of this parameter (usually less than 15 °C). Higher  $\Delta T_1$  gives lower undercooled graphite amount. In the present tested conditions, higher  $\Delta T_1$  level (higher inoculation power) is necessary to limit more the occurrence of this graphite morphology.
- (4) For each tested cooling modulus/solidification cooling rate, the relationship between chill sensitiveness and eutectic undercooling  $\Delta T_1$  parameter evaluated by thermal analysis is stronger than the dependence between chill and inoculant amount addition. Higher  $\Delta T_1$  gives lower chill tendency, independently of inoculant consumption, inoculant type, solidification cooling rate and chill evaluation criteria.
- (5) The present work illustrates the possibility to evaluate the eutectic cells count by standard thermal analysis. Eutectic cells count decreased by increasing of the undercooling referring to stable eutectic temperature ( $\Delta T_m$ ), but increased by increasing of the undercooling referring to metastable eutectic temperature ( $\Delta T_1$ ).

- (6) White iron solidification as intercellular carbides and/or inverse chill and micro-shrinkage occur at the latter part of solidification. A preferred end of solidification means high solidus temperature and low level (less negative) of the  $\Delta T_3$  parameter (usually at low negative value, as  $TES < T_{mst}$  in most cases), especially obtained by inoculation.
- (7) Undercooling degree at the end of solidification ( $\Delta T_3$ ) is in good relationship with the maximum eutectic undercooling at the beginning of eutectic reaction, expressed by its reference to stable eutectic temperature ( $\Delta T_m$ ) and metastable eutectic temperature ( $\Delta T_1$ ), respectively.
- (8) Higher inoculant amount addition gives higher relative density, according to lower undercooling on entire solidification range ( $\Delta T_m$ ,  $\Delta T_1$ ,  $\Delta T_3$ ).
- (9) The mentioned positive effects (lower eutectic undercooling, lower carbides and undercooled graphite amount, and higher eutectic cells count and relative density) characterize each inoculation alloy (inoculant). Generally, rare earth bearing ferrosilicon alloy led to the best results as a decrease of eutectic undercooling for entire eutectic range and carbides sensitiveness, especially at low addition rate.
- (10) The obtained results sustain the possibility to evaluate the chill (carbides formation) tendency and structure characteristics of a specific solidified casting by thermal analysis recorded in standard Quick-cup<sup>TM</sup> conditions.
- (11)  $\Delta T_1$  appears to be the most important cooling curve analysis parameter to characterize the specific of solidification pattern and structure formation on the entire solidification range.
6. Emadi D, Whiting LV, Nafisi S, Ghomashchi R. Applications of thermal analysis in quality control of solidification processes. *J Therm Anal Calorim.* 2005;81:235–42.
7. Dioszegi A, Svensson IL. On the problems of thermal analysis of solidification. *Mater Sci Eng A.* 2005;413–414:474–9.
8. Sillen RV. Novacast Technologies, [www.novacast.se](http://www.novacast.se), 2006.
9. Chisamera M, Stan S, Riposan I, Costache G, Barstow M. Solidification pattern of in-mold and ladle inoculated low sulfur hypoeutectic gray cast irons. *AFS Trans.* 2008;116:641–52.
10. Stan S, Chisamera M, Riposan I, Stefan E, Barstow M. Solidification pattern of un-inoculated and inoculated gray cast irons in wedge test samples. *AFS Trans.* 2010;118:295–309.
11. Sparkman D. Microstructure by Thermal Analysis. *AFS Trans.* 2011; Paper 11-068:413–419.
12. Stan S, Chisamera M, Riposan I, Barstow M. Applications of thermal analysis to monitor the quality of hypoeutectic cast irons during solidification in sand and metal moulds. *J Therm Anal Calorim.* 2012;110(3):1185–92.
13. Stefanescu DM, Moran M, Boonmee S. The use of combined liquid displacement and cooling curve analysis in understanding the solidification of cast iron. *AFS Trans.* 2012;120:365–74.
14. Riposan I, Chisamera M, Stan S, Barstow M. Identifying chill tendency of cast iron melts by thermal analysis. *Int J Cast Met Res.* 2013;26(3):152–9.
15. Alonso G, Stefanescu DM, Suarez R. Understanding graphite expansion during the eutectic solidification of cast iron through combined linear displacement and thermal analysis. *Int Foundry Res.* 2014;66(4):2–12.
16. Riposan I, Stefan IC, Firican MC, Stan S. Thermal Analysis to Optimize and Control the Cast Iron Solidification Process. In: *Proc 6<sup>th</sup> Int Conf. Advanced Materials and Structures–AMS '13*, 16–17 Oct. 2015, Timisoara, Romania.
17. Stefanescu DM. Thermal analysis-theory and applications in metalcasting. *J Metalcasting.* 2015;9(1):7–22.
18. Klancnik U, Habjan J, Klancnik G, Medved J. Thermal analysis of indefinite chill cast iron modified with ferrovanadium and ferrotungsten. *J Therm Anal Calorim.* 2017;127:71–8.
19. Tadesse A, Fredriksson H. Volume change during the solidification of grey cast iron: its relation with the microstructural variation, comparison between experimental and theoretical analysis. *Int J Cast Met Res.* 2017. <https://doi.org/10.1080/13640461.2016.1277851>.
20. Chisamera M, Riposan I, Stan S, Skaland T. Effects of calcium and strontium undercooling, chill and microstructure in grey irons of varying sulphur and oxygen contents. In: *Proc. 64th World Foundry Congress, 2000, Paris, France, Paper No. 62*.
21. Riposan I, Chisamera M, Stan S, Skaland T, Onsoien MI. Analyses of possible nucleation sites in Ca/Sr overinoculated grey irons. *AFS Trans.* 2001;109:1151–62.
22. Riposan I, Chisamera M, Stan S, Skaland T. Graphite nucleants (microinclusions) characterization in Ca/Sr inoculated grey irons. *Int J Cast Metal Res.* 2003; 16(1–3):105–111.
23. Riposan I, Chisamera M, Stan S, Toboc P, Ecob C, White D. Al, Zr-FeSi preconditioning of grey cast irons. *Mater Sci Technol.* 2008;24(5):579–84.
24. Chisamera M, Riposan I, Stan S, White D, Grasmö G. Graphite nucleation control in grey cast iron. *Int J Cast Metal Res.* 2008;21(1–4):39–44.
25. Sommerfeld A, Tonn B. Nucleation of graphite in cast iron melts depending on manganese, sulphur and oxygen. *Int J Cast Met Res.* 2008;21(1–4):23–6.
26. Gundlach R. observations on structure control to improve the properties of cast irons. The honorary cast iron lecture, Div.5, 112nd AFS Metalcasting Congress, Atlanta, Georgia, USA; 2008. Paper 08–158.

**Acknowledgements** This work was partially financed by a grant of the Romanian National Authority for Scientific Research and Innovation, CNCS/CCCDI-UEFISCDI, project number PN-III-P2-2.1-PED-2016-1793, within PNCDI III.

## References

- Riposan I, Chisamera M, Stan S. New developments in high quality grey cast irons. *China Foundry.* 2014;11(4):351–64.
- Riposan I, Skaland T. Modification and Inoculation of Cast Iron. In: In D.M. Stefanescu, Volume Editor, *Cast Iron Science and Technology Handbook.* 2017. pp. 160–176, American Society of Materials.
- Sparkman D, Bhaskaram CA. Chill measurement by thermal analysis. *AFS Trans.* 1996;104:969–76.
- Sillen RV. Optimizing Inoculation Practice by means of Thermal Analysis. In: *AFS International Inoculation Conference*, 6–8 Apr. 1998, Rosemont, Illinois, USA.
- Dioszegi A, Hattel J. Inverse thermal analysis method to study solidification in cast iron. *Int J Cast Met Res.* 2004;17(5):311–8.

27. Riposan I, Chisamera M, Stan S, Ecob C, Wilkinson D. Role of Al, Ti, Zr in Grey Iron Preconditioning/Inoculation. *J Mater Eng Perform*. 2009;18(1):83–7.
28. Sommerfeld A, Tonn B. Theory of graphite nucleation in lamellar graphite cast iron. *Int. J. Metalcasting*. 2009;3(4):39–47.
29. Campbell JA. Hypothesis for cast iron microstructures. *Met Mater Trans B*. 2009;40(6):786–801.
30. Riposan I, Chisamera M, Stan S, Hartung C, White D. Three-stage model for nucleation of graphite in grey cast iron. *Mater Sci Technol*. 2010;26(12):1439–47.
31. Elmquist L, Salera S, Dioszegi A. Inoculation and its effect on primary solidification structure of hypoeutectic grey cast iron. *Int J Cast Met Res*. 2010;23(2):124–9.
32. Riposan I, Chisamera M, Stan S. Enhanced quality in electric melt grey cast irons. *ISIJ Int*. 2013;53(10):1683–95.
33. Alonso G, Stefanescu DM, Larranaga P, De la Fuente F, Suarez R. On the Nucleation of Graphite in Lamellar Graphite Cast Iron. *AFS Trans*. 2016; 124:Paper 16–020.
34. American Society for Testing of Materials, Standard A367–85: Standard Test Methods of Chill Testing of Cast Iron, 1. West Conshohocken. USA: PA; 2000. p. 151–4.
35. Riposan I, Chisamera M, Stan S, White D. Chilling properties of Ba/Ca/Sr inoculated grey cast irons. *Int J Cast Met Res*. 2007;20(2):90–7.